Available online at www.sciencedirect.com

SciVerse ScienceDirect

Journal homepage: **www.elsevier.com/locate/cortex**

ELSEVIER
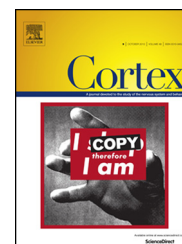
Cortex

Research report

Causal evidence for posterior parietal cortex involvement in visual-to-motor transformations of reach targets

Aarlenne Z. Khan [a,b,d], *Laure Pisella* [b,c] *and Gunnar Blohm* [a,d,*]

[a] *Centre for Neuroscience Studies, Queen's University, Kingston, ON, Canada*
[b] *INSERM U1028, CNRS UMR5292, Lyon Neuroscience Research Center, ImpAct Team, Bron, France*
[c] *Mouvement et Handicap, Hospices Civils de Lyon, Inserm et Université de Lyon, Bron, France*
[d] *Canadian Action and Perception Network (CAPnet), Canada*

ARTICLE INFO

ABSTRACT

It has been posited that the posterior parietal cortex (PPC) is involved in the visual-to-motor transformation for reach planning. Such a transformation is required because in general the retinal information and the arm motor command do not align, for example in the case of non-zero eye/head orientations. Here, we present behavioral data from a patient with unilateral optic ataxia consecutive to damage to the superior parietal lobule including the intraparietal sulcus in the right hemisphere, who we asked to reach to visual targets under different head roll angles. An accurate visual-to-motor transformation has to integrate head roll to compensate for the rotated retinal location of the target, resulting in a head roll-independent pattern of reach endpoints. If however, head roll is not compensated for, reach endpoints should vary across different head rolls, reflecting a reach plan based on the rotated retinal target location. Remarkably, the patient compensated for head roll when reaching to targets presented within his intact right visual field (VF) (not different from controls) but not for reaches to targets in the contralesional left VF. The amount of compensation was the same irrespective of whether the initial hand position was located in the left or right VF, showing that this transformation concerns only the target location and not the hand-target motor vector. We interpret these findings as causal evidence for the involvement of the PPC in integrating head roll signals in the visual-to-motor transformation of the reach target.

1. Introduction

Movement planning requires a sensory-to-motor transformation (Crawford et al., 2004; Snyder, 2000; Soechting and Flanders, 1992). In the case of the visual-to-motor transformation for reaching, visual information enters the brain in retinal coordinates, whereas the arm motor plan needs to be specified in a coordinate system relative to the shoulder, the insertion point of the arm (Flash and Sejnowski, 2001). Therefore, retinal inputs have to be transformed into shoulder-centered coordinates by means of a reference frame transformation that takes the relative misalignment of the

eyes, head and body into account (Blohm and Crawford, 2007; Crawford et al., 2004).

Current views state that this transformation occurs in a distributed parietal–frontal network of areas; correlates of the visual-to-motor conversion for reaching have been shown in the posterior parietal cortex (PPC) (Battaglia-Mayer et al., 2003; Batista et al., 1999; Buneo et al., 2002; Cohen and Andersen, 2002) as well as the dorsal part of the pre-motor cortex (Battaglia-Mayer et al., 2003; Batista et al., 2007; Pesaran et al., 2006). The PPC has long been known as a sensory association area (Hyvarinen, 1982); it receives visual information from striate and extra-striate areas (Robinson et al., 1978) and carries information about eye and head position from pro-prioception (Brotchie et al., 1995), inner ear organs (Andersen et al., 1999) and efference copies of the motor commands (Mountcastle et al., 1975). In addition, neurophysiological recordings in the PPC have shown gain modulation of visual receptive fields by eye and head position signals (Andersen et al., 1985; Brotchie et al., 1995), which is believed to be the signature of reference frame transformations (Blohm and Crawford, 2009). Previous reaching studies on optic ataxia patients with PPC damage (Perenin and Vighetto, 1988) have shown that early internal representations of target location are accurate (Khan et al., 2005b) suggesting that the PPC is involved in reference frame transformations which result in reaching deficits to visual targets. However the causal role of the PPC for a retinal-to-shoulder transformation has never been explicitly tested.

With chronic lesions, a consistent deficit argues strongly for a causal role of an area for a certain process, since plasticity mechanisms have been unable to eliminate the functional deficit even after many years (Rafal, 2006). We asked a patient with chronic left optic ataxia resulting from damage to the superior parietal lobule (SPL) and the intraparietal sulcus (IPS) in the right hemisphere and a group of neurologically intact controls to reach to targets from different initial hand positions (IHPs) while the head was straight or rolled to either shoulder.

We used head roll as a tool to dissociate retinal and shoulder-centered reference frames, allowing us to directly address the role of the PPC in the visual-to-shoulder reference frame transformation for reaching. The advantage of head roll is that it rotates the retinal stimuli around the fovea without compromising their visual quality. Under different head roll orientations, the visual input is rotated around the line of sight, creating a misalignment of visual and shoulder reference frames. This requires a head roll-dependent reference frame transformation to compensate for this misalignment. We evaluated the subjects' ability to compensate for head roll in the visuomotor transformation against our predictions; if head roll was not accounted for at all, we would expect a rotation of reach endpoints that is equal to the rotation of the visual image on the retina, resulting in large head-roll dependent changes in reach endpoints. This is shown in Fig. 1, where the leftward reach target (relative to the shoulder – Fig. 1A) is rotated relative to the retinal axes when the head is rolled to the left (Fig. 1B). Our tilted reaching setup is depicted in Fig. 1C, which results in targets being projected in a specific manner onto the reaching surface. Thus, if the head is straight, the reach target is projected directly to the left
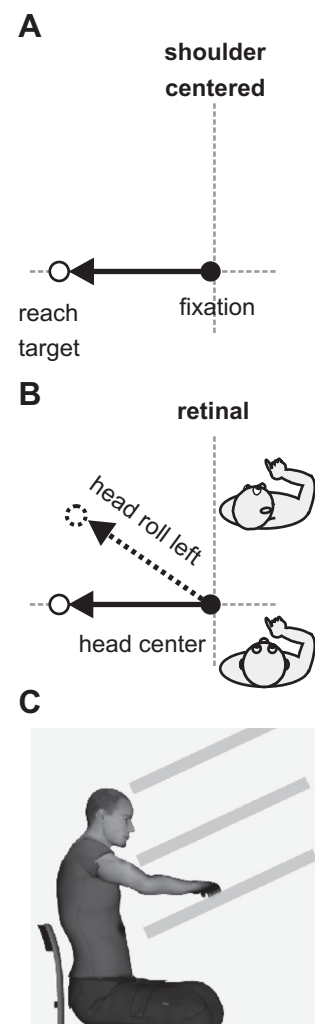
Fig. 1 — Schematic of hypothesis. A. In a shoulder-centered reference frame, the leftward reach target (open circle) is directly left of the fixation (black filled circle) regardless of head roll as shown by the arrow. The dotted lines represent the cardinal axes relative to the shoulder. B. However, in a retinal reference frame, the location of the reach target changes depending on head roll. If the head is at center, the reach target direction matches that of the shoulder-centered reference frame (solid arrow). However, when the head is rolled toward the left shoulder (as in the upper icon), the direction of the reach target relative to the cardinal axes changes (dotted arrow). C. Depiction of the tilted reaching setup. Subjects viewed targets projected from the top surface, through a half-reflecting mirror (middle surface) onto a tilted reaching surface. All surfaces were tilted 30°. Through this setup, subjects reached to targets without visual feedback of their hand.

of the fixation (open solid circle in Fig. 1B). However, if the head is rolled to the left and head roll is not compensated for, the reach would be shifted to the target's retinal position (open dotted circle) which is projected further in depth on the reaching surface, i.e., the subject would reach to the target's retinal position as if the head was upright. In contrast, when

the head is rolled to the right, the target's retinal would be projected closer in depth. Alternatively, if head roll was fully accounted for then we predict no systematic shift of reach endpoints with head roll.

In addition, we analyzed the influence of changes in IHPs on the amount of head roll compensation. We hypothesized that if only the reach target underwent the reference frame transformation, then IHP should not affect the head roll compensation errors. If however it was the desired movement vector that was transformed, then IHP should have an effect on the compensation errors. This is because reaching from the left IHP would entail a motor vector that is at least partially encoded in the right PPC (depending on the reach target location), while reaching from the right IHP would constitute greater involvement of the left PPC. Therefore, unilateral damage to PPC should differentially affect the amount of head roll compensation for left versus right IHPs if the desired movement vector was transformed, whereas there should be no differences in head roll compensation across different IHPs if it was only the reach target that underwent the reference frame transformation.

2. Methods

2.1. Subjects

Patient C.F. (denoted as CF from now on) is a right-handed 33-year-old male who suffered from a watershed posterior infarct, 7 years before testing, resulting in multiple asymmetrical bilateral lesions of the occipital and parietal regions (Fig. 2A). Lesions were mainly located in the right anterior SPL (Brodmann's areas 2, 5 and 7), the right anterior IPS and the lateral and middle occipital gyri bilaterally (Brodmann's areas 18 and 19). The left IPS was entirely preserved as well as the bilateral parieto−occipital junction (POJ), inferior parietal lobule (IPL) and temporal−parietal junction (TPJ). The patient did not exhibit any purely motor, somatosensory or visual deficits or any sign of neglect shown through a set of standard clinical tests including visual field (VF) topography, sensory stimulation tests and evaluation of reflexes and muscle tone and joint movements. He shows chronic left unilateral optic ataxia, with larger deviations and variability for reaches to targets presented in the left VF and in central vision using the right hand (Khan et al., 2005b, 2007) and to targets in both VFs using the left hand (Blangero et al., 2008).

Five age-matched control subjects also took part in this study (ages: 31−42, M = 35, SD = 4.3). All subjects had normal or corrected-to-normal vision and gave informed consent to participate in the experiment according to the French law (4th March 2002) on human subjects' rights.

2.2. Apparatus

Subjects were seated in front of a tilted table (30°) on which they performed reaching movements using their right hand. The subject's head was supported by on a chin rest. Two tilted side headrests were located on either side of the chin rest rotated to 30° left and right from vertical. A light-emitting diode (LED) target array was located above the table and was
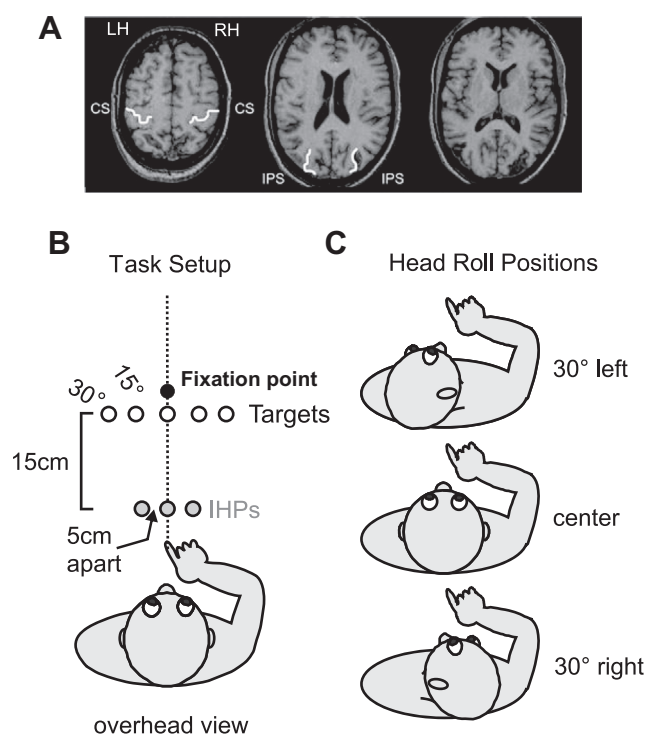
Fig. 2 − Magnetic resonance imaging slices of patient CF and task setup. A. T1 scans for patient CF. The dark areas at the bottom of the scans show damage to the dorsal occipital and the superior parietal cortices, which is larger and extends to the IPS in the right hemisphere.
CS = central sulcus, RH = right hemisphere, LH = left hemisphere. B. Task setup. Subjects reached from one of three IHPs (gray filled circles). The center IHP was always illuminated regardless of which IHP the subject started from. Subjects reached to the remembered position of one of five reach targets (white filled circles) in complete darkness while fixating at the central fixation point (black circle). C. Head roll positions. Subjects reached to targets after rolling their head to one of three positions (30° toward the left shoulder, upright (center), or 30° toward the right shoulder) as directed through auditory instructions.

projected onto it using a half-reflecting mirror, such that they were able to see the target array but not their hand during reaching. The LED array consisted of an IHP LED (IHP − center gray filled circle in Fig. 2B) aligned to the mid-sagittal plane (vertical dotted line) located 5 cm in front of the subject's torso. Two additional IHPs were located 5 cm right and left of the center IHP LED (gray filled circles) but were not visible to the subject. Five reaching targets (white filled circles) were aligned horizontally 15 cm in front of the IHP LED and located at 30° left, 15° left, 0°, 15° right, 30° right. A fixation LED was located 1 cm above the central reach target LED (black filled circle).

Movements of the right index finger were sampled at 1000 Hz using an Optotrak 3020 (NDI, Waterloo, Ontario, Canada) infrared marker-based motion tracking system. Eye movements were recorded binocularly at 50 Hz using a DC electrooculograph (EOG) system (Biomedica Mangoni, Pisa,

Italy) by placing electrodes outside the lower left and upper right eyes.

2.3. Task

At the beginning of each trial, the central IHP LED was illuminated. The experimenter positioned the subject's index finger to one of the three randomly selected IHPs (Fig. 2B − gray filled circles). Then, the IHP LED was extinguished and the fixation LED was illuminated. Subjects were instructed to fixate on this LED. After 500 msec, an audio voice informed subjects of the required head position (left, right or upright − Fig. 2C). When rolling the head left or right, subjects were asked to lean the side of their head on the respective tilted headrest. Next, one of the five reach target LEDs was illuminated for 500 msec. Subjects were asked to reach to the target as soon as it was extinguished while looking at the fixation LED throughout. The trial ended with the extinction of the fixation LED 500 msec after the end of the reach movement (calculated online).

2.4. Data analysis

We collected three blocks from each control and four from CF (two repetitions * three head rolls * three IHPs * five reach targets within each block), resulting in a total of 1710 trials. 3.2% (55 trials) of trials were removed because of missing Optotrak data (CF − 10%, controls 0−5.2%). In addition, 3.8% (65 trials) were removed because subjects made an eye movement during the trial (CF 6.4%, controls .4−11.5% − see Fig. 3D for an example). The beginning and end of reach movements were detected based on a velocity criterion (80 mm/sec). Start and end positions of the reaching movement were sampled 50 msec before the onset and after the offset of the reach movement respectively. All trials were visually inspected to ensure accuracy of detection. To ensure a reliable measure of consistent reach endpoints, we removed trials with absolute distances that were greater than 3SD away from the mean for each target, head roll and subject. We removed nine trials in total (.6%).

CF was compared against the control group using modified *t*-tests (Crawford and Garthwaite, 2002); these are designed specifically to test whether single subject's (patient) data falls within the range of control data, using the control group's mean and standard deviation (SD). They provide a robust comparison of a single data point against a small group of controls for single case studies. For tests within subjects, we used separate analysis of variance tests (ANOVA) for each individual subject.

Data are represented in coordinates defined by the tilted reach surface (Fig. 1B) and relative to the subject's view, i.e., *X*-axis is left−right, *Y*-axis is close−far (in depth) parallel to the surface and *Z*-axis is orthogonal to the reach surface. To measure the amount of compensation for the head roll, we calculated a head roll compensation index, which is an index (regression slope) comparing the predicted reach errors if head roll was not compensated for at all to the actual reach errors produced in the surface−depth axis (*y* position). Predicted reach errors were calculated as the target distance from fixation multiplied by the sine of the head roll angle projected onto the tilted surface, resulting in a y position of −70 mm (closer to the participant) for right head roll and 70 mm

(further away) for left head roll compared to 0 for the head straight position. If the subject did not compensate for head roll at all, the index (slope) would equal 1, whereas if they perfectly compensated for head roll, the slope would equal 0.

3. Results

3.1. Movement parameters

To provide the reader a better intuition about the data and in order to ensure that our main findings did not result from abnormal sensory processing or motor control, we first analyzed basic movement parameters. Fig. 3A shows traces of the reach and eye movements from a typical trial performed by CF. After the offset of the reach target (vertical dotted line), CF performed a movement to the 30° leftward reach target as can be seen by the x, y and z positions of the index finger plotted against time. The corresponding eye position from the amplified EOG signal is also shown. As can be seen, CF maintained position at the central fixation target during the entire trial. Fig. 3B shows this trial (red) along with a trial (orange and green) to each different reach target location (black crosses) in an above view, with x position (left vs right relative to the subject) plotted against y position (close vs far from the subject, i.e., in depth parallel to the reach surface). As can be seen, CF typically overshot the target locations in depth, but this is not different from neurologically intact subjects in conditions using half-reflecting mirrors (Khan et al., 2005a). The same trials are plotted in Fig. 3C in the side view with y position plotted against z position (on vs above the table surface). As can be noted, CF's reaching endpoints are different when pointing to targets in his left (damaged) VF (red and orange traces) compared to targets in central vision or in the right (intact) VF (green traces).

To contrast this good trial with one removed from the analysis, Fig. 3D shows a trial during which CF made an eye movement to the target. While he performed an appropriate reaching movement to the 30° leftward reach target, he made an eye movement to the target before the reach movement and then returned to the fixation spot. We removed these trials from the analysis.

Erroneous sensory processing should result in abnormal reaction times (RT). To analyze this, Fig. 3E shows cumulative frequencies for reach RT for CF (blue trace) as well as each control subject (gray traces). As can be seen, CF as well as three control subjects tended to anticipate the offset of the reach target (2nd vertical dotted line). Since subjects had no visual feedback of their reaching movement, the presence of the reach target was inconsequential. Essentially, the timing of their reaching movements was not important. A modified *t*-test comparing the patient to the group of controls showed no significant differences [$t(1) = .76$, $p > .05$], showing that CF's RTs were well within the range of the control RTs.

Finally, we verified that CF did not have abnormal motor control. Fig. 3F shows movement duration plotted as a function of peak velocity for CF (blue dots) and controls (other colored dots) as well as histograms for each kinematic. As is generally the case, peak velocity decreased as movement duration increased, both for CF and for controls. Statistical
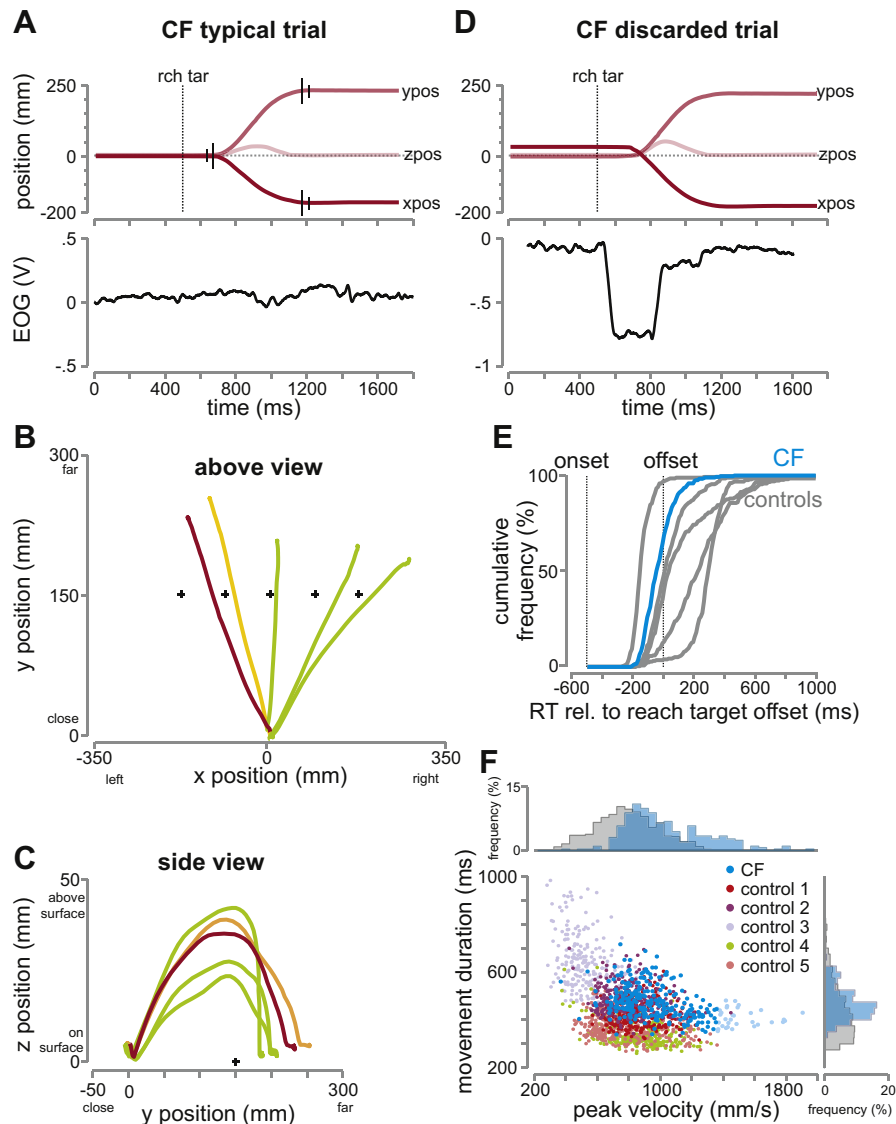
Fig. 3 — **Typical trials and reach parameters. A. Typical trial for CF reaching to a 30° leftward target. The top panel shows traces for x, y and z position plotted over time (in msec). The vertical dotted line shows the time at which the reach target was extinguished, signaling subjects to reach. The longer of the small solid vertical lines represent the onset and offset of the reach movement, as determined the velocity criterion (80 mm/sec). The shorter lines represent the point at which the start and the endpoints of the reach movements were extracted (50 msec before/after reach onset/offset). The lower panel shows amplified EOG traces (in Volts) recorded from the eyes. In this trial, CF remained fixated at the center fixation position throughout without moving his eyes. B. CF example reaches in above view. The typical trial in A (in red) along with four other reach movements (orange — to the 15° leftward target, green — to the central and rightward targets) to each of the five different reach targets (shown by black crosses) are depicted from an above view. Y position (position in depth, where 0 is close to the subject and 300 is far) is plotted against x position (left is negative/right is positive). C. Side view. The same trials are shown from a side view, where z position (position in height, where 0 is on the table surface and 50 is above the surface) is plotted against y position (depth). D. Example discarded trial from CF. The figure is depicted in the same manner as A. While CF performed an appropriate reach movement to the same 30° leftward target, he made an eye movement to the reach target just before/during the reach movement (bottom panel). Therefore, this trial was removed from the analysis. E. RTs. Cumulative frequencies (in percentages) of RT are shown for CF (blue) as well as controls (gray). In the x-axis are RTs relative to reach target offset (2nd vertical dotted line). Reach onset is also shown (1st dotted vertical line). F. Reach kinematics. Movement duration (msec) is plotted against peak velocity (mm/sec) for CF (blue dots) as well as controls (other colored dots, see legend). The corresponding frequency histograms for duration (right) and peak velocity (top) are also shown across all controls together (gray) and separately for CF (blue).**

analyses using modified *t*-tests (see data analysis section) showed no differences between CF and the controls for either peak velocity [$t(1) = 1.6$, $p > .05$] or movement duration [$t(1) = .14$, $p > .05$]. Comparing the relationship between movement duration and peak velocity, we found that CF's slope ($-.122$) was well within the range of controls ($-.332$ to $.034$). As can be seen, there are a few trials where the peak velocity is higher for CF than controls (highlighted in lighter blue, $N = 33$, 11% of CF's trials). We confirmed that in terms of reach endpoint in depth, there was no difference between these specific trials and all other trials ($p > .05$). Also, they were equally distributed across the three head rolls.

3.2. Reach endpoints

Fig. 4 shows individual reach endpoints for the patient CF (**A**) and a control subject (**B**). Data for the three head roll orientations are shown in different colors (blue: head rolled to right shoulder; green: head straight; red: head rolled to left
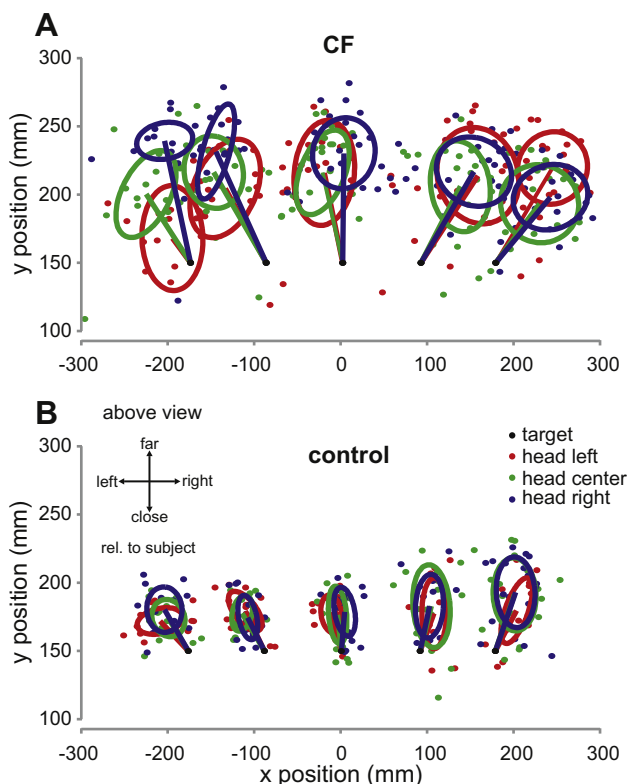
Fig. 4 – Reach endpoints across all trials for CF and a control subject (above view). A. Reach endpoints in mm relative to the center IHP are plotted for CF color coded by head roll position (head left = red, head center = green, head right = blue). Actual target positions are shown by the black dots. The colored lines connect the mean position for each head roll and target to the corresponding target location. The ellipses are 1 SD ellipses centered on the mean position; the two main axes of the two-dimensional reach endpoints were computed using eigenvectors of the covariance matrix and then the 1 SD points were determined along these axes. B. Reach endpoints for a typical control.

shoulder) pooled across all IHPs. It can be seen that there is a difference in reach endpoints in depth (*y* position) across head roll orientations, mainly for targets in the left (impaired) VF; the SD ellipses change position for different head orientations. A shift in *y* position/depth with head roll would be predicted if head roll was not taken into account (Fig. 1B/D).

For CF, a two-factor ANOVA, with head roll and VF as factors and *y* position (depth) as the dependent measure revealed a significant effect of head roll [$F(2,158) = 11.9$, $p < .01$] but no effect of VF ($p > .05$). There was a significant interaction effect [$F(2,158) = 3.3$, $p < .05$], showing that the effect of head roll was greater in the left VF (both leftward reach targets together: mean *y* position head left = 188 mm; head straight = 209; head right = 235) than in the right VF (both rightward reach targets together: head left = 217 mm, head straight = 199, head right = 207). In summary, CF shows a systematic head-roll dependent shift in *y* reach endpoint position only in the left (affected) VF.

For proper comparison to CF, we also performed two-factor ANOVAs for the control subjects, however no consistent VF differences are expected. We did find significant differences between VF for two control subjects, however they showed opposite patterns [sub 1: $F(1, 152) = 32$, $p < .001$, mean *y* position left VF = 162 mm, right VF = 150, sub 4: $F(1,153) = 34$, $p < .001$, left VF = 160 mm, right VF = 172]. For head roll, three of the five subjects showed significant effects, however these did not vary systematically with head roll position and in addition were very small [sub 2: $F(2,152) = 6$, $p < .01$, mean *y* position head left = 153, head straight = 153, head right = 163; sub 4: $F(2,155) = 6.5$, $p < .01$, head left = 190 mm, head straight = 193, head right = 201; sub 5: $F(2,153) = 4.8$, $p < .05$, head left = 131 mm, head straight = 131, head right = 142], as one would typically expect for imperfect head roll compensation (Blohm and Crawford, 2007; Leclercq et al., 2012). Note that this was also the case for CF in the right VF. Finally, one subject showed no significant effects ($p > .05$, Fig. 4B). In summary, only CF showed large linear changes in *y* position that depended on head roll and only in the left VF (significant interaction effect between VF and head roll), as would be expected if head roll was not fully compensated for, due to the right SPL/IPS lesion.

3.3. Head roll compensation

We computed a head roll compensation error as an index of the accuracy of the reference frame transformation. Using regression analysis, we compared the predicted reach endpoints if movement planning did not account for head roll to actual reach endpoints in depth (*y* position). Fig. 5A plots CF's reach endpoints for the 30° leftward target (gray dots) as a function of the predicted target retinal shift for the three head roll orientations. The predicted retinal shift of the target was calculated to be approximately $+/-70$ mm when the head was tilted to the left/right respectively. Thus, a regression fit with a slope of 1 corresponds to the error predicted if head roll was not taken into account, and movement planning was purely based on the target's retinal direction (retinal prediction), whereas a slope of 0 means that reach endpoints were spatially accurate, fully
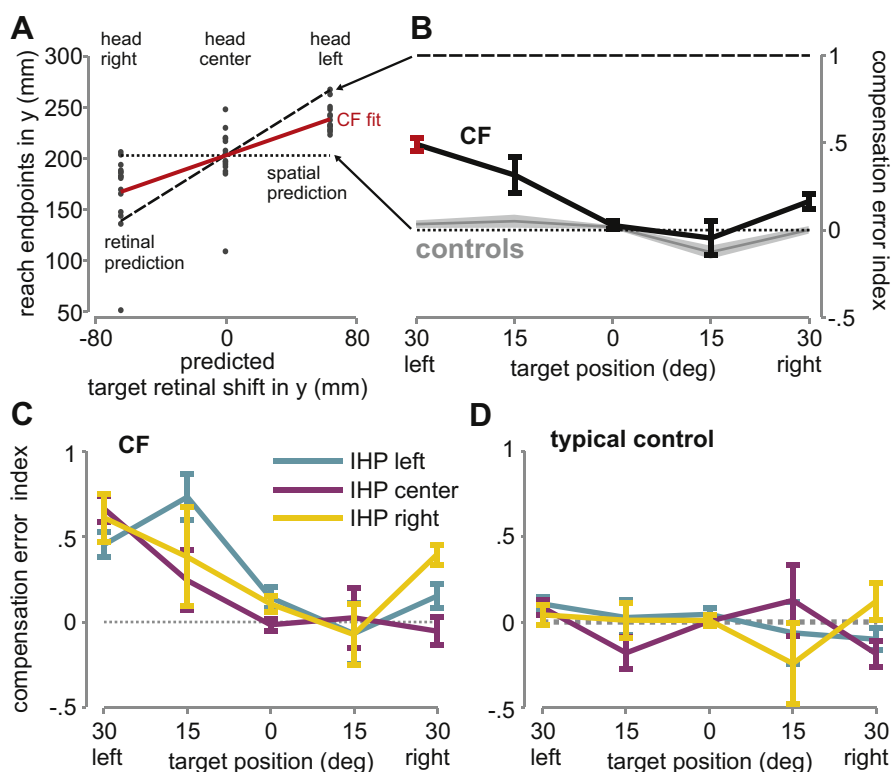
Fig. 5 – Compensation error index. A. Regression analysis for 30° leftward target across the three head rolls for CF. Actual reach endpoints in y were plotted against the predicted target retinal shift (as in **Fig. 1**B) for each of the three head rolls (head right is on the left side, head center and head left − on the right − in gray). The horizontal dotted line represents the spatial prediction, i.e., the head roll is perfectly accounted for and so there is no change in reach endpoint for the three head rolls. The dashed diagonal line represents the retinal prediction, i.e., the reach endpoints are entirely determined by the reach target positions on the retina. The fit to the reach endpoints for CF is shown in red. B. Compensation error indices, i.e., slopes for the regression fits from A, for CF (red data point from A, otherwise black) and across all controls (gray) for the five different target positions. The arrows from the y-axis show the corresponding values from A. The error bars for CF are standard error of the mean (SEM) across trials; the error windows (gray) for the controls are SEM across the five controls. C. Compensation error indices for CF separated by IHPs. D. Compensation error indices for a typical control.

compensating for the retinal–spatial misalignment (spatial prediction). The regression fit to the CF's data (in red) shows that for this target, CF only partially compensated for the head roll orientation.

Fig. 5B shows the regression slopes (compensation error index) across the five reach target locations for CF (red = 30° leftward target shown in Fig. 5A) and the group of controls. As can be seen, controls almost perfectly compensated for head roll. In contrast, while CF showed similar compensation performance for targets presented in his intact right VF, he showed a much higher compensation error for targets in his impaired left VF, only compensating for about 50% of head roll. Modified t-tests on the compensation error revealed significant differences between CF and controls for the targets in the left [collapsed across the two targets, CF = .49, controls = .09 (SD = .08), $t(1) = 4.2$, $p = .013$] but not in the right VF [CF = −.05, controls = .06 (SD = .12), $p > .05$].

Fig. 5C and D shows the head roll compensation index separately for all three IHP conditions for patient CF and our typical control subject respectively. We did not observe any significant differences of the compensation index across

IHPs for either CF [$F(2,12) = .1$, $p > .05$] or any control subject ($p > .05$). These results suggest that it is only the reach target position and not the movement vector that undergoes the reference frame transformation for reaching in PPC.

4.   Discussion

We show that a unilateral optic ataxia patient following damage to the right SPL/IPS shows faulty compensation for head roll during reaching for targets in his left (affected) VF, while reaches to targets in the right (intact) VF did not change depending on head roll orientations. In addition, we did not observe any influence of IHP. Based on these results, we conclude that SPL/IPS region is directly and causally involved in integrating head roll position signals for the retinal-to-shoulder reference frame transformation of the visual target location for reaching.

Previous imaging (Beurze et al., 2010; Medendorp et al., 2005), electrophysiological (Batista et al., 1999; Buneo et al.,

2002; Cohen and Andersen, 2002) and patient (Blangero et al., 2007, 2010; Buxbaum and Coslett, 1997, 1998; Dijkerman et al., 2006; Khan et al., 2005a, 2007) studies have focussed on the reference frame of reach coding in parietal cortex and have demonstrated that visual and proprioceptive information of the hand and target are mainly coded in gaze-centered co-ordinates. The fact that many PPC neurons are gain-modulated by eye and head orientation signals (Andersen et al., 1985; Brotchie et al., 1995; Chang et al., 2009) and that reach-related signals in pre-motor and motor areas seem to code reaches in effector-centered coordinates (Kakei et al., 2001; Kalaska et al., 1997; Scott, 2003; Pesaran et al., 2006) has led to the belief that PPC is involved in reference frame transformations (Crawford et al., 2004; Snyder et al., 1997; Snyder, 2000). This has been based on mathematical modeling studies demonstrating that gain modulation by eye/head orientation gaze-centered receptive fields within the PPC can result in effector-centered receptive field properties in areas downstream such as the pre-motor cortex (Blohm et al., 2009; Pouget and Sejnowski, 1997; Salinas and Abbott, 2001; Zipser and Andersen, 1988). In addition, patient studies have also provided some evidence of the involvement of the PPC in reference frame transformation by showing changes in reaching patterns with changes in head, torso and hand po-sitions (Jax et al., 2009; Khan et al., 2007). However, no patient or animal lesion study has specifically examined the ability to integrate different head roll orientations in reach planning following PPC damage.

One possibly surprising finding is that patient CF compensated for about 50% of head roll, which could be interpreted as some partial reference frame transformation abilities preserved in the right PPC. However, it is likely that this is an overestimation of the actual compensation left. During head roll, the eyes counter-roll in their orbits typically between 5 and 25% in the opposite direction to the head roll (Bockisch and Haslwanter, 2001), leading to a smaller required reference frame transformation than the actual head roll. Due to the side headrests, subjects achieved a head roll angle of 30° or less. Because of ocular counter-roll and head roll restrictions, subjects likely had to compensate for smaller retinal–spatial misalignments. As a consequence, we overestimated the predicted reach endpoints since we based them on the targeted head roll angle of 30° and did not as-sume any counter-roll, leading to an underestimation of head roll compensation index. Nevertheless, if patient CF did retain some reference frame transformation abilities, this could be because these reference frame transformations are carried out in a distributed parietal–frontal network of neu-rons (Blohm et al., 2009) or because the damage to the right PPC is incomplete (POJ, IPL and the caudal part of the SPL/IPS remain undamaged).

Previous studies on optic ataxia patients have shown deficits in reaching movements to visual targets as well as to proprioceptive targets, i.e., the other unseen index finger (Khan et al., 2007; Blangero et al., 2007; Pisella et al., 2009), which has been interpreted as the PPC encoding the hand-target movement vector. Thus, we were interested in whether the reference frame transformation in PPC was carried out on the visual target position only or rather on the movement vector. We predicted that if target position alone

was transformed using head orientation signals, then the reach endpoints should be unaffected by IHP; alternatively, if the movement vector was transformed as a whole, we pre-dicted an interaction effect of head roll and IHP on reach endpoints. This is because if the representation of IHP was lateralized in PPC (Beurze et al., 2010), then we would expect different reach endpoints (and head roll compensation) when reaches were initiated from the left versus right VF. We found that the IHP had no effect on reach endpoints or head roll compensation; the target position alone was affected by a faulty reference frame transformation. This finding is compatible with previous ones on patients with PPC lesions (who exhibit independent and additive visual and hand effects: review in Pisella et al., 2009), which suggest that hand and target are processed separately within the PPC (Blangero et al., 2011) and combined at further stage (e.g., pre-motor). This is also the case for neurophysiological studies in non-human primates (Buneo et al., 2002; Chang et al., 2008; Chang and Snyder, 2012; Pesaran et al., 2006). Indeed, it has been demonstrated that while both and target information is present in area PPC, they are not combined to form a motor plan in the PPC, but rather in pre-motor cortex (Buneo et al., 2002; Pesaran et al., 2006). Consistent with current neural network studies (Blohm et al., 2009; Pouget et al., 2002), eye position gain modulations found in PPC (Chang et al., 2009; Chang and Snyder, 2010, 2012) of yet uncombined hand and target signals are the required inter-mediate processing signatures that produce spatial motor plans in pre-motor cortex (Blohm and Crawford, 2009; Crawford et al., 2004; Pouget and Snyder, 2000). Thus, our results are consistent with this literature showing indepen-dent hand and target coding in PPC. In addition, hand posi-tion information has been shown to be less lateralized and more distributed in PPC compared to the hand that is used (Beurze et al., 2010). As such, unilateral damage would still preserve some initial right hand position information in the unaffected (left) PPC, which could then be transformed correctly independently of target position. The combination of the hand and target would then occur downstream of the PPC lesion, in pre-motor or motor areas.

In conclusion, we found that a patient with unilateral optic ataxia had a deficit in compensating for head roll only when reaching to targets in his impaired VF (left VF corresponding to damage in the right SPL/IPS) and that this faulty compensa-tion remained the same regardless of IHP. This demonstrates that SPL/IPL is causally involved in integrating head roll po-sition signals into the retinal-to-shoulder transformation of the reach target.

REFERENCES

Andersen RA, Essick GK, and Siegel RM. Encoding of spatial location by posterior parietal neurons. *Science*, 230(4724): 456–458, 1985.

Andersen RA, Shenoy KV, Snyder LH, Bradley DC, and Crowell JA. The contributions of vestibular signals to the representations of space in the posterior parietal cortex. *Annals of the New York Academy of Science*, 871: 282–292, 1999.

Batista AP, Buneo CA, Snyder LH, and Andersen RA. Reach plans in eye-centered coordinates. *Science*, 285(5425): 257–260, 1999.

Batista AP, Batista AP, Santhanam G, Yu BM, Ryu SI, Afshar A, and Shenoy KV. Reference frames for reach planning in macaque dorsal premotor cortex. *Journal of Neurophysiology*, 98(2): 966–983, 2007.

Battaglia-Mayer A, Caminiti R, Lacquaniti F, and Zago M. Multiple levels of representation of reaching in the parieto–frontal network. *Cerebral Cortex*, 13(10): 1009–1022, 2003.

Beurze SM, Toni I, Pisella L, and Medendorp WP. Reference frames for reach planning in human parietofrontal cortex. *Journal of Neurophysiology*, 104(3): 1736–1745, 2010.

Blangero A, Gaveau V, Luauté J, Rode G, Salemme R, Guinard M, et al. A hand and a field effect in on-line motor control in unilateral optic ataxia. *Cortex*, 44(5): 560–568, 2008.

Blangero A, Khan AZ, Rode G, Rossetti Y, and Pisella L. Dissociation between intentional and automatic remapping: Different levels of inter-hemispheric transfer. *Vision Research*, 51(8): 932–939, 2011.

Blangero A, Ota H, Delporte L, Revol P, Vindras P, Rode G, et al. Optic ataxia is not only 'optic': Impaired spatial integration of proprioceptive information. *NeuroImage*, 36(Suppl. 2): T61–T68, 2007.

Blangero A, Ota H, Rossetti Y, Fujii T, Ohtake H, Tabuchi M, et al. Systematic retinotopic error vectors in unilateral optic ataxia. *Cortex*, 46(1): 77–93, 2010.

Blohm G, Keith GP, and Crawford JD. Decoding the cortical transformations for visually guided reaching in 3D space. *Cerebral Cortex*, 19(6): 1372–1393, 2009.

Blohm G and Crawford JD. Computations for geometrically accurate visually guided reaching in 3-D space. *Journal of Vision*, 7(5): 4 1–422, 2007.

Blohm G and Crawford JD. Fields of gain in the brain. *Neuron*, 64(5): 598–600, 2009.

Bockisch CJ and Haslwanter T. Three-dimensional eye position during static roll and pitch in humans. *Vision Research*, 41(16): 2127–2137, 2001.

Brotchie PR, Andersen RA, Snyder LH, and Goodman SJ. Head position signals used by parietal neurons to encode locations of visual stimuli. *Nature*, 375(6528): 232–235, 1995.

Buneo CA, Jarvis MR, Batista AP, and Andersen RA. Direct visuomotor transformations for reaching. *Nature*, 416(6881): 632–636, 2002.

Buxbaum LJ and Coslett HB. Spatio-motor representations in reaching: Evidence for subtypes of optic ataxia. *Cognitive Neuropsychology*, 15: 279–312, 1998.

Buxbaum LJ and Coslett HB. Subtypes of optic ataxia: Reframing the disconnection account. *Neurocase*, 3: 159–166, 1997.

Chang SWC, Dickinson AR, and Snyder LH. Limb-specific representation for reaching in the posterior parietal cortex. *Journal of Neuroscience*, 28: 6128–6140, 2008.

Chang SWC, Papadimitriou C, and Snyder LH. Using a compound gain field to compute a reach plan. *Neuron*, 64: 744–755, 2009.

Chang SW and Snyder LH. Idiosyncratic and systematic aspects of spatial representations in the macaque parietal cortex. *Proceedings of the National Academy of Sciences*, 107(17): 7951–7956, 2010.

Chang SW and Snyder LH. The representations of reach endpoints in posterior parietal cortex depend on which hand does the reaching. *Journal of Neurophysiology*, 107(9): 2352–2365, 2012.

Cohen YE and Andersen RA. A common reference frame for movement plans in the posterior parietal cortex. *Nature Reviews Neuroscience*, 3(7): 553–562, 2002.

Crawford JD, Medendorp WP, and Marotta JJ. Spatial transformations for eye–hand coordination. *Journal of Neurophysiology*, 92(1): 10–19, 2004.

Crawford JR and Garthwaite PH. Investigation of the single case in neuropsychology: Confidence limits on the abnormality of test scores and test score differences. *Neuropsychologia*, 40: 1196–1208, 2002.

Dijkerman HC, McIntosh RD, Anema HA, de Haan EH, Kappelle LJ, and Milner AD. Reaching errors in optic ataxia are linked to eye position rather than head or body position. *Neuropsychologia*, 44(13): 2766–2773, 2006.

Flash T and Sejnowski TJ. Computational approaches to motor control. *Current Opinion Neurobiology*, 11(6): 655–662, 2001.

Hyvarinen J. Posterior parietal lobe of the primate brain. *Physiology Review*, 62(3): 1060–1129, 1982.

Jax SA, Buxbaum LJ, Lie E, and Coslett HB. More than (where the target) meets the eyes: Disrupted visuomotor transformations in optic ataxia. *Neuropsychologia*, 47(1): 230–238, 2009.

Kakei S, Hoffman DS, and Strick PL. Direction of action is represented in the ventral premotor cortex. *Nature Neuroscience*, 4(10): 1020–1025, 2001.

Kalaska JF, Scott SH, Cisek P, and Sergio LE. Cortical control of reaching movements. *Current Opinion in Neurobiology*, 7(6): 849–859, 1997.

Khan AZ, Crawford JD, Blohm G, Urquizar C, Rossetti Y, and Pisella L. Influence of initial hand and target position on reach errors in optic ataxic and normal subjects. *Journal of Vision*, 7(5)(8): 1–16, 2007.

Khan AZ, Pisella L, Rossetti Y, Vighetto A, and Crawford JD. Impairment of gaze-centered updating of reach targets in bilateral parietal–occipital damaged patients. *Cerebral Cortex*, 15(10): 1547–1560, 2005a.

Khan AZ, Pisella L, Vighetto A, Cotton F, Luauté J, Boisson D, et al. Optic ataxia errors depend on remapped, not viewed, target location. *Nature Neuroscience*, 8(4): 418–420, 2005b.

Leclercq G, Blohm G, and Lefèvre P. Accurate planning of manual tracking requires a 3D visuomotor transformation of velocity signals. *Journal of Vision*, 12(5): 6, 2012.

Medendorp WP, Goltz HC, Crawford JD, and Vilis T. Integration of target and effector information in human posterior parietal cortex for the planning of action. *Journal of Neurophysiology*, 93(2): 954–962, 2005.

Mountcastle VB, Lynch JC, Georgopoulos A, Sakata H, and Acuna C. Posterior parietal association cortex of the monkey: Command functions for operations within extrapersonal space. *Journal of Neurophysiology*, 38(4): 871–908, 1975.

Perenin MT and Vighetto A. Optic ataxia: A specific disruption in visuomotor mechanisms. I. Different aspects of the deficit in reaching for objects. *Brain*, 111(3): 643–674, 1988.

Pesaran B, Nelson MJ, and Andersen RA. Dorsal premotor neurons encode the relative position of the hand, eye, and goal during reach planning. *Neuron*, 51(1): 125–134, 2006.

Pisella L, Sergio L, Blangero A, Torchin H, Vighetto A, and Rossetti Y. Optic ataxia and the function of the dorsal stream: Contributions to perception and action. *Neuropsychologia*, 47(14): 3033–3044, 2009.

Pouget A, Deneve S, and Duhamel JR. A computational perspective on the neural basis of multisensory spatial representations. *Nature Reviews Neuroscience*, 3: 741–747, 2002.

Pouget A and Sejnowski TJ. A new view of hemineglect based on the response properties of parietal neurones. *Philosophical*

Transactions of the Royal Society of London. Series B, Biological Sciences, 352(1360): 1449—1459, 1997.

Pouget A and Snyder LH. Computational approaches to sensorimotor transformations. *Nature Neuroscience*, 3: 1192—1198, 2000.

Rafal RD. Oculomotor functions of the parietal lobe: Effects of chronic lesions in humans. *Cortex*, 42(5): 730—739, 2006.

Robinson DL, Goldberg ME, and Stanton GB. Parietal association cortex in the primate: Sensory mechanisms and behavioral modulations. *Journal of Neurophysiology*, 41(4): 910—932, 1978.

Salinas E and Abbott LF. Coordinate transformations in the visual system: How to generate gain fields and what to compute with them. *Progress in Brain Research*, 130: 175—190, 2001.

Scott SH. The role of primary motor cortex in goal-directed movements: Insights from neurophysiological studies on non-human primates. *Current Opinion in Neurobiology*, 13(6): 671—677, 2003.

Snyder LH. Coordinate transformations for eye and arm movements in the brain. *Current Opinion in Neurobiology*, 10(6): 747—754, 2000.

Snyder LH, Batista AP, and Andersen RA. Coding of intention in the posterior parietal cortex. *Nature*, 386(6621): 167—170, 1997.

Soechting JF and Flanders M. Moving in three-dimensional space: Frames of reference, vectors, and coordinate systems. *Annual Review of Neuroscience*, 15: 167—191, 1992.

Zipser D and Andersen RA. The role of the teacher in learning-based models of parietal area 7a. *Brain Research Bulletin*, 21(3): 505—512, 1988.